Received: 21 June 2017 | Revised: 20 November 2017 | Accepted: 13 December 2017

DOI: 10.1111/gcb.14036

PRIMARY RESEARCH ARTICLE

WILEY Global Change Biology

Chronosequence predictions are robust in a Neotropical secondary forest, but plots miss the mark

Justin M. Becknell[1,2] | Stephen Porder[2,3] | Steven Hancock[4] | Robin L. Chazdon[5] | Michelle A. Hofton[4] | James B. Blair[6] | James R. Kellner[2,3]

[1]Environmental Studies Program, Colby College, Waterville, ME, USA

[2]Institute at Brown for Environment and Society, Brown University, Providence, RI, USA

[3]Department of Ecology and Evolutionary Biology, Brown University, Providence, RI, USA

[4]Department of Geographical Sciences, University of Maryland, College Park, MD, USA

[5]Department of Ecology and Evolutionary Biology, University of Connecticut, Storrs, CT, USA

[6]NASA Goddard Space Flight Center, Greenbelt, MD, USA

Correspondence
Justin M. Becknell, Environmental Studies Program, Colby College, Waterville, ME, USA.
Email: justin.becknell@colby.edu

Abstract

Tropical secondary forests (TSF) are a global carbon sink of 1.6 Pg C/year. However, TSF carbon uptake is estimated using chronosequence studies that assume differently aged forests can be used to predict change in aboveground biomass density (AGBD) over time. We tested this assumption using two airborne lidar datasets separated by 11.5 years over a Neotropical landscape. Using data from 1998, we predicted canopy height and AGBD within 1.1 and 10.3% of observations in 2009, with higher accuracy for forest height than AGBD and for older TSFs in comparison to younger ones. This result indicates that the space-for-time assumption is robust at the landscape-scale. However, since lidar measurements of secondary tropical forest are rare, we used the 1998 lidar dataset to test how well plot-based studies quantify the mean TSF height and biomass in a landscape. We found that the sample area required to produce estimates of height or AGBD close to the landscape mean is larger than the typical area sampled in secondary forest chronosequence studies. For example, estimating AGBD within 10% of the landscape mean requires more than thirty 0.1 ha plots per age class, and more total area for larger plots. We conclude that under-sampling in ground-based studies may introduce error into estimations of the TSF carbon sink, and that this error can be reduced by more extensive use of lidar measurements.

KEYWORDS
biomass, La Selva, Land Vegetation and Ice Sensor, secondary succession, tropical forest, waveform lidar

1 | INTRODUCTION

Tropical secondary forests (TSF) are increasing in area and account for as much as 59% of all tropical forests (FAO 2015), and recent estimates suggest they are a carbon sink of around 1.6 Pg C/year (Pan et al., 2011). Both numbers are likely to increase in the coming decades (Chazdon, 2014). Secondary succession in tropical forests takes decades to occur, and thus understanding the trajectory of recovery is rarely studied in real time. Rather, predictions of changes in forest height and aboveground biomass density (AGBD) are based on chronosequence studies that substitute space for time, that is, use contemporaneous forests of different ages to quantify change over time (Aide, Zimmerman, Pascarella, Rivera, & Marcano Vega, 2000; Becknell & Powers 2014; Johnson & Miyanishi, 2008; Letcher & Chazdon, 2009). Thus, our understanding of the TSF carbon sink, as well as predicted forest structural changes, depends on the validity of the assumption that space-for-time substitutions can accurately and precisely predict AGBD change.

Until recently, testing this assumption has been infeasible because repeated measurements of regenerating forests over large areas have not been available. Some TSF plots have been surveyed over multiple years (Rozendaal & Chazdon, 2015; Rozendaal et al.,

2017), but the effort involved means that the sample sizes for such studies are small. Furthermore, if the goal of chronosequence studies is to estimate the landscape distribution of forest recovery, repeated measures of plots may not be adequate if the chosen plot is not representative of the true (unquantified) landscape distribution. In the absence of decades long studies at the landscape-scale, we do not know whether it is reasonable to assume, for example, that a 10-year-old forest will grow, in the coming decade, to resemble an adjacent 20-year-old forest. A second concern is that the reality of working in secondary-forest landscapes can preclude random sampling and sufficient replication to characterize the mean state of different forest ages. Regenerating TSF landscapes are comprised of small patches of differing stand ages that make large plots difficult to locate and replicate (Chazdon, 2003).

Despite these limitations, data from existing TSF suggest rapid accumulation of AGBD early in secondary succession, reaching 90% of old-growth forest AGBD in 66 years on average in the Neotropics (Poorter et al., 2016). However, within the Neotropics, secondary forest AGBD in 20-year-old forests varies by more than an order of magnitude, from 25 to 200 Mg/ha with outliers as high as 500 Mg/ha (Poorter et al., 2016). Annual precipitation explains some of this variation, as wetter forests accumulate AGBD faster, but substantial variation remains even among sites with little variation in precipitation (Aide et al., 2000; Becknell & Powers, 2014; Letcher & Chazdon, 2009). This variation in AGBD may be due to differences in tree communities, soils, or land-use history (Chazdon, 2003; Kennard, 2002; Lasky et al., 2014). It is also possible that they result from stochastic processes such as weather or disturbance (Arroyo-Rodríguez et al., 2015; Norden et al., 2015). Finally, it may be that the typical sampling effort to quantify AGBD is insufficient to capture the true distribution in heterogeneous TSF landscapes. For example, in mature tropical forest, Marvin et al. (2014) suggest that at least 10 ha of total sample area is needed to estimate AGBD within 90% of the landscape mean. More broadly, efforts to test chronosequences find that their predictions are not always borne out (Feldpausch, da Conceicao Prates-Clark, Fernandes, & Riha, 2007; Johnson & Miyanishi, 2008; Maza-Villalobos, Balvanera, & Martínez-Ramos, 2011; Mora et al., 2014). However, it is not clear whether discrepancies between chronosequence predictions and observations over time are because the predictions are flawed, trajectories of TSF succession are inherently unpredictable, and a larger sample is needed to obtain a better estimate of forest trajectories, or some combination of these factors.

These results raise questions of global relevance. Should we expect rapid AGBD accumulation across most TSFs in the coming decades? Or will there be large variance among regions? Is the rate of AGBD accumulation in a particular TSF landscape more likely to follow the Neotropical mean path or one elucidated by a particular plot-based chronosequence from that landscape? Finding the ecological drivers of the variation in forest recovery will help to answer these questions. But finding those drivers will be challenging if part or most of the variation is the result of a violation of the assumptions embedded in chronosequence-based predictions (Johnson & Miyanishi, 2008) or if sample sizes among studies of TSF succession are insufficient (Getzin, Fischer, Knapp, & Huth, 2017; Marvin et al., 2014; Poorter et al., 2016).

In this context, we asked whether predictions from chronosequences are robust when evaluated using repeated landscape-scale measurements from airborne lidar in a Neotropical secondary forest around La Selva Biological Station in the Atlantic lowlands of Costa Rica. We used airborne lidar collected in 1998 over forests of different ages (0–10, 11–20, 21–30 years) to predict the change in forest height and AGBD. We tested these predictions 11.5 years later using data from a second airborne lidar survey, enabling a direct, landscape-scale test of space-for-time assumption that underlies all chronosequence studies. Since repeated lidar surveys are still rare in the tropics, we also used these data to ask whether sampling typical of TSF chronosequence studies is likely to produce estimates of mean height and AGBD that are close to the landscape mean. We do this by repeatedly taking plot-sized samples of lidar data and comparing the simulated plot means to estimates of the landscape mean from airborne lidar.

2 | MATERIALS AND METHODS

The study was conducted in tropical wet forest at La Selva Biological Station in the Atlantic lowlands of Costa Rica (Figure 1). The site is 41–142 m above sea level and receives 4 m of precipitation

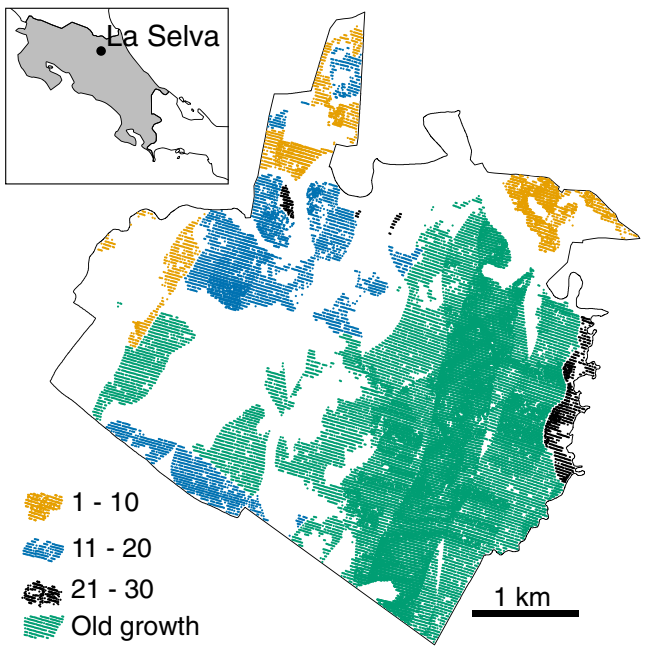

FIGURE 1 Map of La Selva Biological Station in Northeastern Costa Rica (inset). Circles represent Land Vegetation and Ice Sensor (LVIS) footprints in forests of different age classes in 1998. Orange, blue, and black circles are in secondary forest. Green circles are in old-growth forest. Areas with no circles either have no LVIS footprints or were excluded because they were in experimental areas, former plantations, or selectively logged forest

annually. The study area includes both old-growth (778 ha) and secondary forests (340 ha), the latter mostly on low-lying alluvial terraces, and the former on both alluvial terraces and upland Oxisols. Mean annual temperature is 26°C and rainfall exceeds 200 mm in every month. A detailed site description is in McDade, Bawa, Hespenheide, and Hartshorn (1993).

2.1 | Mapping forest age

We determined the age of secondary forest using a time series of aerial photos acquired in 1966, 1971, 1976, 1983, 1988, and 2005 and expert knowledge of local land-use history. We georeferenced aerial photos and manually digitized forest and non-forest areas. Forests were defined as areas with ≥50% tree cover with a minimum mapping unit of 0.25 ha. This classification produced a time series of secondary forest areas with known dates of origination. We classified each area using four age classes: 1–10 years, 11–20 years, 21–30 years, and old-growth forest, where age classes represent status in 1998. We used the land-cover map in Kellner, Clark, and Hofton (2009) to identify and exclude riparian areas, selectively logged areas, developed areas, experimental plots, and forest plantations.

2.2 | Airborne lidar data

We used data from two lidar sensors collected 11.5 years apart to quantify canopy height changes and AGBD. In March 1998, NASA's Land Vegetation and Ice Sensor (LVIS) large-footprint waveform lidar instrument collected data from an altitude of 8 km, which produced nominal footprint diameters of 25 m at ground level. The LVIS sensor digitizes the vertical distribution of intercepted surfaces illuminated within every laser footprint. Each waveform was sampled using 0.3 m vertical bins and geographically projected relative to the WGS1984 ellipsoid using the International Terrestrial Reference Frame. We re-projected the LVIS data into UTM zone 16 N. In September 2009, a small footprint commercial lidar (discrete return lidar—DRL) was used to collect measurements over the same area. We describe our method for comparing these two datasets below.

2.3 | Simulating waveform lidar data from DRL data

Throughout our analysis, we describe analyses based on recorded LVIS waveforms and simulated waveforms derived from DRL. We use the term "waveform" to refer to recorded LVIS waveforms. We adopt the terminology of Blair and Hofton (1999) and refer to simulated waveforms derived from DRL as "pseudo-waveforms." The 2009 DRL data were collected by an Optech 3100EA lidar sensor in September, 2009, from an altitude of 1.5 km, resulting in a mean point density of 3.5 per m^2 (Neumann, Saatchi, & Clark, 2012; TEAM Network 2009). DRL sensors typically produce a small laser footprint of up to a few tens of cm in diameter. These sensors use proprietary algorithms to determine and record a number of discrete ranges from the returned laser energy to produce a point cloud. Although some commercial lidar sensors record the entire distribution of returned laser energy (the waveform), the full waveform is normally not retained. This sensor recorded up to four discrete returns for every emitted laser pulse. Maps of canopy height, forest structure, and AGBD derived from lidar data at this site are available in Drake, Dubayah, Clark, and Knox (2002), Neumann et al. (2012), Dubayah et al. (2010), and Thomas, Kellner, Clark, and Peart (2013).

We chose to compare these particular datasets because, to our knowledge, this is the longest time interval between two lidar measurements of secondary forest anywhere in the tropics. However, small-footprint DRL and large-footprint waveform measurements are not directly comparable without additional processing. Fortunately, DRL measurements closely match waveforms recorded by LVIS when the LVIS pulse width and along-beam pulse length are applied to the DRL point cloud (Blair & Hofton, 1999). We used this approach to produce pseudo-waveforms from the 2009 lidar data that can be directly compared with LVIS waveforms (Figure 2).

The equation for a pseudo-waveform, y, is:

$$y(z) = \sum_{i=1}^{m} \sum_{j=1}^{n} e^{-d_j^2/2\sigma_f^2} e^{-\left(z_i - h_j\right)^2/2\sigma_p^2} \quad (1)$$

The equation contains kernels for two Gaussian distributions, which represent the distribution of intensity along or across the beam path, with half-widths of $\sigma_f = 0.6893$ and $\sigma_p = 6.25$ m, respectively (Blair & Hofton, 1999). Nominal footprint diameter is $4\sigma_p = 25$ m. The summations are over m vertical elevation bins at which the pseudo-waveform is sampled, and n reflective surfaces (DRL points) within the waveform footprint. z_i is the elevation of the ith vertical bin, and h_j is the elevation of the jth DRL point within the footprint of the pseudo-waveform. The variable d_j^2 is the squared horizontal distance in meters between each DRL point and the center of the pseudo-waveform.

2.4 | Correcting for vertical and horizontal offsets between lidar datasets

For the LVIS waveforms from 1998 and pseudo-waveforms from the 2009 DRL data to be comparable, we had to identify and correct vertical or horizontal offsets between the two datasets. We quantified the Easting and Northing offset between the 1998 and 2009 lidar data sources using "bullseye plots" (Blair & Hofton, 1999). The method works by choosing a random sample of 1,000 LVIS waveforms in old-growth forest, and then produces pseudo-waveforms from the 2009 DRL data using Equation (1) at the same Easting and Northing locations. We then computed the correlation coefficient between each pseudo- and recorded waveform, and stored the mean across the 1,000 random samples. Next, we shifted the location of the pseudo-waveforms in the Easting or Northing axes by a small increment, computed correlation coefficients, and stored the mean. By repeating this process for all combinations of Easting and Northing offsets from −10 to 10 m in increments of 1 m, one can produce a plot of the correlation coefficient as a function of the Easting and Northing offsets. The values of the Easting and Northing offsets that maximize the correlation coefficient define the systematic

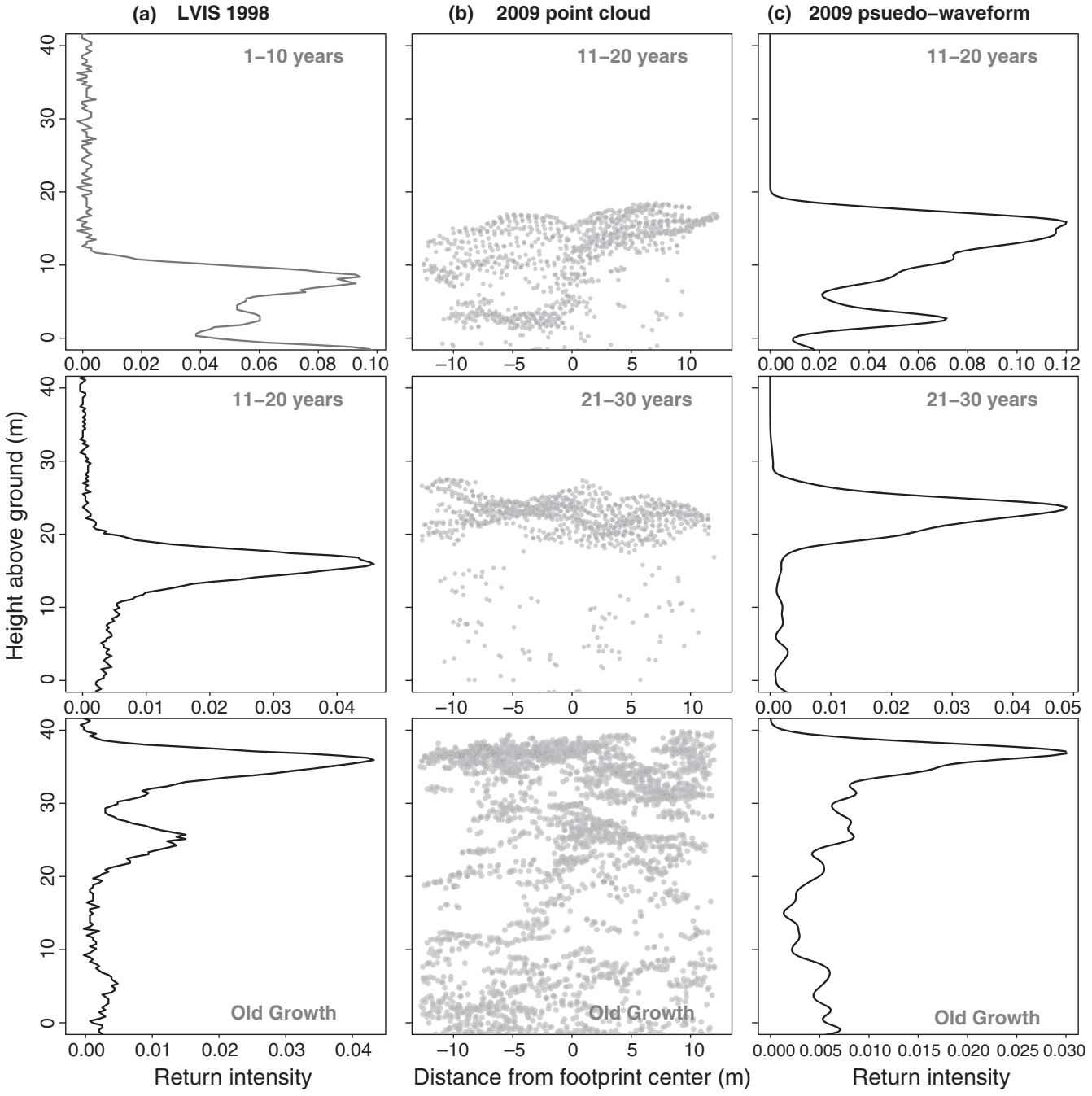

FIGURE 2 Waveforms, discrete-return point clouds, and pseudo-waveforms from secondary and old-growth forests in the Atlantic lowlands of Costa Rica. Each row represents a single footprint from the 1998 Land Vegetation and Ice Sensor (LVIS) data. The left column (a) shows waveforms from the original LVIS data collected in 1998. The middle column (b) shows discrete return lidar (DRL) point clouds from 2009 within the extent of the LVIS waveform. The third column (c) shows pseudo-waveforms generated from the DRL point cloud that allow for comparison between the 1998 and 2009 data. Because there were no forests aged 31–40 years in 1998, our analysis considers the transitions between 1–10 and 11–20 years, and between 11–20 and 21–30 years

difference between two data sources. If the data are perfectly co-registered, the maximum correlation coefficient is when the Easting and Northing offsets are 0. These analyses demonstrated that there is an Easting offset of 4 m and a Northing offset of 1 m. We applied Easting and Northing offsets to the 1998 LVIS Easting and Northing locations. This allowed us to produce pseudo-waveforms at the corrected locations for 45,144 LVIS waveforms using Equation (1).

To determine whether there is a vertical offset between data sources, we identified LVIS waveforms in areas that were flat, open pastures in 1998 and 2009. We did this because it eliminates Easting and Northing offsets as a source of variation, and because computing the vertical offset within a forested landscape, as opposed to a flat area like a pasture, requires the falsifiable assumption that mean canopy height was constant over time. For example, two

recent studies of canopy height changes at La Selva detected a 0.29 m decrease in mean canopy height (Dubayah et al., 2010; Kellner, Clark, & Hubbell, 2009). Bullseye plots would lead to the conclusion that this change is a spurious offset, when in fact it is probably a real change. Therefore, we selected 494 LVIS waveforms within pastures. We then computed the variance of the DRL elevations within the extent of each LVIS footprint. If the variance was <0.5 m, we used the particular LVIS waveform to evaluate the vertical offset. Otherwise, we inferred that there were objects within the footprint of the LVIS waveform in 2009 other than flat pasture and we rejected the waveform. For the 85 waveforms retained by this analysis, we produced a pseudo-waveform at the Easting and Northing locations of the LVIS waveform. As for the horizontal offsets, we then shifted the vertical reference frame of each waveform in small increments. For each vertical shift, we computed the mean correlation coefficient between LVIS and pseudo-waveforms. We then plotted the correlation coefficient as a function of the vertical offset. The resulting distribution of vertical offsets among the 85 waveforms overlapped zero (mean = 0.48 m, range = −0.26 to 1.09 m). Because the vertical offset is small and overlaps 0, we did not apply a vertical offset correction. However, our conclusions are qualitatively unchanged by the existence of this vertical offset, whether it is corrected or not.

2.5 | Calculating canopy height and estimating AGBD

To compute waveform height aboveground, we extracted the ground elevation from a digital terrain model (DTM) at the coordinate locations of each footprint center (Kellner, Clark, & Hofton, 2009). We then subtracted the ground elevation from the elevation of each waveform bin. After performing these analyses on all 45,144 waveforms, we normalized the area under the curve of each waveform by dividing each bin by the waveform sum. We added noise to pseudo-waveforms by sampling the noise distribution from the top 20 m of corresponding LVIS waveforms. Examination of sensor noise in LVIS waveforms indicates that it is well characterized by a Gaussian distribution. We determined the standard deviation of these distributions and then added Gaussian noise with a mean of 0 and the corresponding standard deviation to each pseudo-waveform. We used each pair of waveforms at the same location separated in time by 11.5 years to quantify canopy height changes and to test predictions for canopy height changes derived from static observations across the chronosequence using the 1998 LVIS data. Canopy height was calculated as the height of the 99th percentile of the normalized 1998 LVIS waveforms and the maximum DRL height within the footprint for the 2009 pseudo-waveforms.

There are 45,144 LVIS footprints with coincident 2009 airborne lidar (Figure 1). To ensure that our estimates of canopy height and AGBD are spatially representative and statistically independent, we generated 1,000 non-overlapping samples from the set of 45,144 footprints. To produce these samples, we selected a random footprint and then eliminated all footprints within 25 m of the selected footprint center. We repeated this process until there were no overlapping footprints remaining. We repeated this process 1,000 times, resulting in 1,000 random samples of non-overlapping footprints. These samples contained 8,752–8,901 footprints. The mean number of footprints in each age class was 759 (1–10 years), 1,459 (11–20 years), 247 (21–30 years), and 6,366 in old-growth forest.

We computed AGBD (Mg/ha) using a relationship that was derived using the 1998 LVIS data within old-growth and secondary forest at the same site (Drake et al., 2002):

$$\log(\text{AGBD}) = 3.58 + 0.07 \times \text{HOME} \quad (2)$$

HOME is the height of median waveform energy (i.e., the 50th percentile of waveform height). This equation has a coefficient of determination of 0.53, and a root mean-squared error of 63.17 Mg/ha.

2.6 | Testing chronosequence predictions

To test the validity of the space-for-time assumption, we generated summary histograms of canopy height and AGBD from each of the 1,000 non-overlapping footprint samples. We compared the means and distributions of canopy height and AGBD within forests in a given age class in 1998 to forests in the same age class in 2009. These comparisons between predicted and observed canopy height and AGBD enable a direct test of the space-for-time assumption. Because we used data from 1998 to develop predictions, we refer to height and AGBD in 1998 within a given age class as predicted height and AGBD for that age class. We tested these predictions by comparing them to what we call "observed" height and AGBD in forests of the same age class 11.5 years later—forests that were 11.5 years younger in 1998. For example, using measurements from 1998, we quantified height and AGBD for forests aged 11–20 years. If the space-for-time substitution is correct, forests aged 11–20 years in 2009 (which were aged 1–10 years in 1998) should have the same height and AGBD as the forest aged 11–20 years in 1998.

2.7 | Simulated plots

Most estimates of secondary succession are not based on landscape-scale assessments from remote sensing, but rather a small number of plots. To determine whether a given sample of plots can provide a precise, unbiased estimate of the landscape mean canopy height and AGBD, we simulated plot samples using the set of 1,000 non-overlapping LVIS footprints. We did this by randomly sampling clusters of footprints, where cluster sizes of 1, 2, 5, and 10 footprints correspond to plot areas of 0.05, 0.1, 0.25, and 0.5 ha. These sizes are representative of plots frequently used to quantify secondary succession (Poorter et al., 2016). We placed a buffer around each plot to ensure that separate plots were independent, as they would be in a field study. The buffer sizes were 40, 60, 80, and 100 m, respectively. For each plot size, we sampled the number of plots required to cover up to 10 ha. These numbers are 200, 100, 40, and 20 plots,

respectively. For each plot size, we computed the mean canopy height and AGBD for all areas sampled between the area of a single plot and 10 ha. We compared these estimates to the landscape mean from airborne lidar, and we computed the probability that the canopy height or AGBD estimate was within 10% or 20% of the landscape mean.

2.8 | Analysis of the meteorological record

The space-for-time substitution is based on the assumption that space and time are exchangeable. The analysis described above addresses the spatial component of this assumption because we are using geographically distinct locations that represent forests in different age classes. However, chronosequence predictions based on the space-for-time assumption can also fail if conditions before and after the initial measurements are not the same. In our analysis, this could occur if conditions during the 11.5 years prior to the first observation in 1998 were different from the 11.5 years after the first observation and prior to the re-measurement in 2009. We evaluated this possibility by summarizing a daily meteorological record collected at La Selva Biological Station. We aggregated daily precipitation (mm) and solar radiation (MJ) to monthly sums, and daily minimum temperature to monthly means. We compared the monthly distributions of these quantities during the 138 months before and after the first observation in March, 1998 using *t* tests. All analyses were conducted using R (R Development Core Team, 2017).

3 | RESULTS

3.1 | Space-for-time substitutions

Predictions from the space-for-time assumption closely matched observations 11.5 years later (Table 1, Figure 3). We predicted that 1- to 10-year-old forest in 1998 would increase in height from 15.1 m in 1998 to 24.1 m in 2009. The observed mean canopy height in 11- to 20-year-old forest in 2009 was 23.1 m. This is a predicted change of 9.0 m and an observed change of 8.0 m (Figure S1). Similarly, using measurements in 1998, we predicted that forest in the 21–30 years age class in 2009 would have a mean canopy height of 28.0 m (Figure 3). The observed value in 2009 was 28.3 m—a predicted change of 3.9 m and an observed change of 4.2 m (Figure S1).

TABLE 1 Predicted and observed changes in landscape-scale forest height and aboveground biomass density (AGBD). Quantities are means over 1,000 non-overlapping footprint samples of Land Vegetation and Ice Sensor (LVIS) footprints in each age class. Range represents the minimum and maximum mean height or AGBD in single non-overlapping samples of LVIS footprints. There was no 1- to 10-year-old forest in 2009

		Height (m)		Aboveground biomass density (Mg/ha)	
Age class	Year	*M*	Range	*M*	Range
1–10	1998	15.1	14.7–15.4	62.3	60.8–63.7
11–20	1998	24.1	23.9–24.3	106.2	104.4–107.5
11–20	2009	23.1	22.8–23.3	96.3	94.5–98.1
21–30	1998	28.0	27.6–28.5	135.5	129.8–141.4
21–30	2009	28.3	28.2–28.5	132.9	131.4–134.6

These results are from comparisons between the two lidar datasets without correcting for a potential vertical offset. Because the distribution vertical offset estimates overlapped zero, we did not apply the estimated vertical offset mean (0.48 m). If we had applied this offset, LVIS heights would be reduced by 0.48 m. This reduces the predicted heights in the 11–20 and 21–30 age classes from 24.1 and 28.0 to 23.6 and 27.6 m, respectively. In the 11–20 age class, the difference between predictions and observations decreases from 1 m to 0.52 m, and in the 21–30 age class, the difference between predictions and observations increases from 0.3 m to 0.78 m. We thus conclude that the existence of a 0.48 m vertical offset has a negligible impact on conclusions about the space-for-time substitution.

Patterns in predicted and observed AGBD were similar but had greater uncertainty. AGBD was calculated using HOME, which is correlated with canopy height ($r = .82$, $p < .001$; Drake et al., 2002). For forests 11- to 20-years old in 1998, mean AGBD was 106.2 Mg/ha. In 2009, mean AGBD in the 11- to 20-year-old forest was 96.3 Mg/ha, which means a prediction based on 1998 data would result in a 10.3% over-prediction. In the 21–30 age class, AGBD in 1998 was 135.5 Mg/ha, and in 2009 it was 132.9 Mg/ha, so a prediction in 1998 would result in only a 2% over-prediction (Figure S2).

To assess the temporal, rather than spatial, variation that might drive the differences in predicted and observed height or AGBD, we summarized the meteorological record for the decade before and after the 1998 lidar collection. Analysis of the meteorological record indicates that precipitation, solar radiation, and temperature were stable during this time. The mean monthly precipitation during the 138 months before and after the first lidar measurement in March, 1998 were marginally significantly different (334 mm/month prior to the first measurement; 381 mm/month after the first measurement, $p = .04$). There was no significant difference in monthly radiation (438 MJ/month before versus 432 MJ/month after, $p = .5$), and there was no significant difference in the monthly mean of daily minimum temperature (21.6°C before versus 21.8°C after, $p = .1$).

3.2 | Simulated plots

Simulated inventory plots in secondary forest were unlikely to produce estimates of canopy height or AGBD that were close to the landscape mean values unless larger sample sizes were used than are typical in TSF plot studies. The sample size needed to achieve a given degree of accuracy varied with the size of the simulated plots, the age of the forest, and whether AGBD or canopy height was being estimated (Figure 4). In general, small plots required smaller overall sample areas compared to larger plots for a given degree of accuracy, and younger forests required larger sample sizes than older forests. For example, 42 0.1 ha plots (4.2 ha total) in 1- to

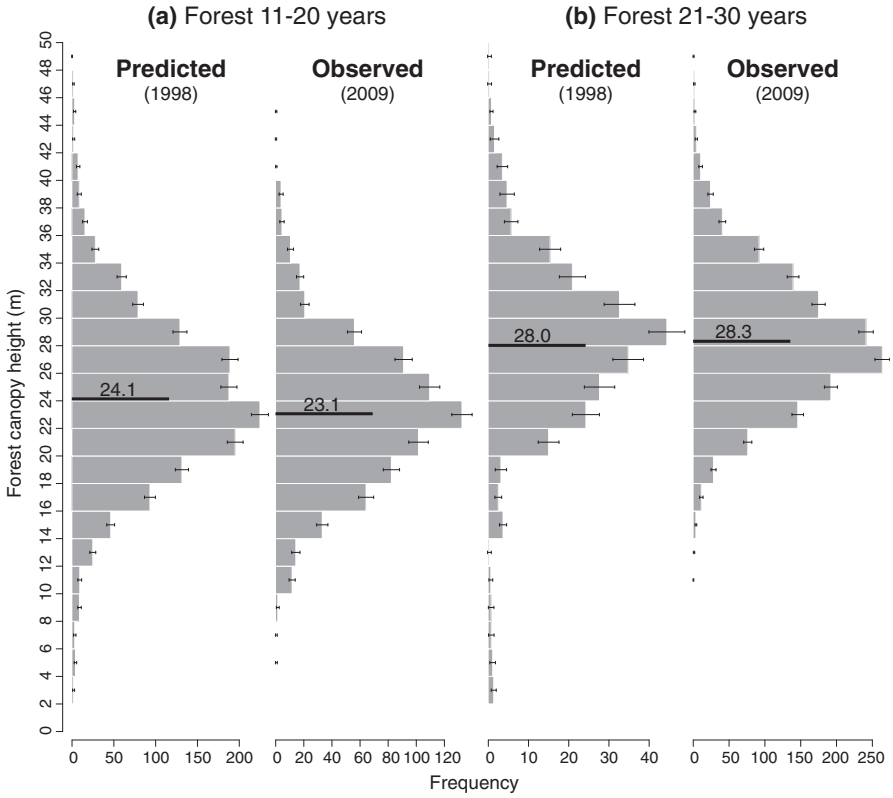

FIGURE 3 Predicted and observed canopy-height distributions for 11–20 (a) and 21–30 (b) year old forest. Each histogram represents the mean of all histograms from 1,000 non-overlapping samples (error bars are standard deviation). Predicted distributions are the distributions of canopy height quantified by Land Vegetation and Ice Sensor in 1998. Observed canopy-height distributions are from 2009 discrete return lidar. Black lines represent the mean of each distribution. The 1- to 10-year age class is omitted from this figure because there were no 1- to 10-year-old forests in the 2009 dataset

10-year-old forests are needed to estimate AGBD within 10% of the landscape mean. Achieving the same degree of accuracy with 0.25 ha plots requires 27 plots (total 6.75 ha). In 11- to 20-year-old forest, estimating AGBD within 10% of the landscape mean requires 39 0.1 ha plots (3.9 ha total). Furthermore, more plots (or area) were required to estimate landscape mean AGBD than height to a given degree of accuracy. For example, in 11- to 20-year-old forest, estimating AGBD within 10% of the landscape mean requires 39 0.1 ha plots, but achieving this same level of accuracy for canopy height requires only 15 plots (1.5 ha).

Old-growth forest required 3.1–5 ha (depending on the plot size used) of total sampling area to estimate AGBD within 10% of the landscape mean (Figure 4). For the same level of accuracy, forest 1- to 10-years old or 11- to 20-years old required 3–9 ha of total sampling area depending on the plot size used. For canopy height in old-growth forest, producing an estimate within 10% of the landscape mean required much smaller sample sizes, just 0.55–1 ha of sampling area depending on the plot size used. In forest 11- to 20-years old, 1–4.5 ha of total sample area are needed to estimate canopy height within 10% of the landscape mean. In contrast, forest 1- to 10-years old required sample sizes comparable to those needed for AGBD to estimate canopy height within 10% of the landscape mean: 3–10 ha depending on the plot size used.

4 | DISCUSSION

Data from airborne lidar collected at two different times across a secondary forest chronosequence in the Atlantic lowlands of Costa Rica show that the space-for-time substitution accurately and precisely predicts canopy height and AGBD during TSF succession. Using lidar data collected in 1998, we predicted that canopy height and AGBD in forests 1- to 10-years old would increase from 15.1 m and 62.3 Mg/ha to 24.1 and 106.2 Mg/ha, respectively. The observations were 23.1 m and 96.3 Mg/ha in 2009 (within 4.3% and 10.3% of our predictions). Our predictions for 11- to 20-year-old forests were that canopy height and AGBD would increase from 24.1 m and 106.2 Mg/ha to 24.8 m and 135.5 Mg/ha, respectively. The observations in 2009 were within 1.1 and 1.8% of the predictions based on 1998 data.

Our findings also demonstrate that small samples typical of field studies of secondary succession in regenerating forests are unlikely to produce estimates close to the landscape mean. Simulated plot samples of the four sizes we considered (0.05, 0.1, 0.25, and 0.5 ha) always resulted in estimates that were asymptotically unbiased (Figure 4). But the variance was large enough that little confidence could be placed in these estimates. For example, repeatedly sampling a simulated chronosequence with 5 0.1 ha plots per age class (a not unreasonable number for an on-the-ground chronosequence sample) 1,000 times demonstrates that any given estimate of the landscape mean AGBD is likely to differ from the landscape value by >10%, 51%–55% of the time (depending on the age class). The likelihood that the sample mean differs from the landscape value by >10% increases with plot size when the total area sampled is fixed. A consequence of this sampling error is that predictions based on the space-for-time substitution derived from small numbers of plots along TSF chronosequences are unlikely to be close to the true value. Chronosequence estimates of change between age classes

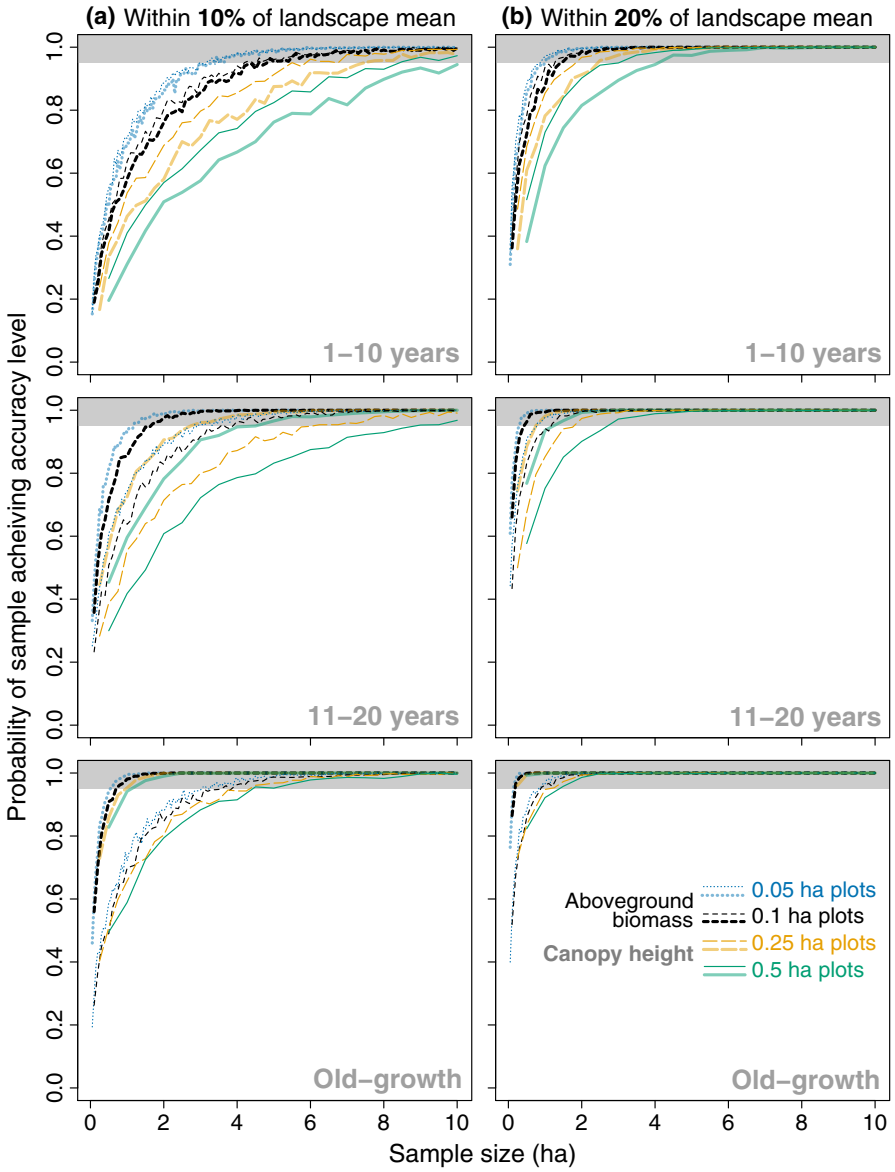

FIGURE 4 Effects of plot size and number on the probability of achieving an estimate within 10% (a) or 20% (b) of the landscape mean value for height (thick light lines) or AGBD (thin dark lines). We simulated samples of different numbers of plots for each plot size (0.05, 0.1. 0.25, and 0.5 ha) made up of randomly selected clusters of non-overlapping of Land Vegetation and Ice Sensor footprints. We did not perform a simulation for forest aged 21–30 years because the sample size was too small. Lines represent the portion of 1,000 simulated sets of plots for each plot size and number of plots whose mean height or AGBD was within 10 or 20% of the landscape mean. The *X*-axis is the sample size in hectares, and depends on the number of plots used in each simulation. Colors represent plot sizes. Shaded areas represent a 95% or greater probability. When the area sampled is equivalent, larger plots are more likely to produce erroneous estimates than smaller plots. Values represented by each line are listed in Table S1 [Colour figure can be viewed at wileyonlinelibrary.com]

could compound this error by combining erroneous estimates from multiple age classes. Furthermore, these results represent the best-cast scenario because few field plots in secondary tropical forest are located randomly because of logistical issues such as access to sites, patch size, and land ownership. We emphasize that the extent to which plots fail to generate robust predictions about the trajectory of TSFs in this study is due to limits in statistical power, rather than violations of the space-for-time assumption because the predictions from landscape-scale lidar are accurate.

4.1 | Sources of uncertainty in secondary succession

Non-random variation in secondary succession could undermine the space-for-time substitution due to violations of the spatial component, or because conditions before and after initial measurement are not the same. The 1998 ENSO resulted in elevated frequencies of canopy damage in old-growth forest at this site that are anomalous during the subsequent 12 years (Silva, Kellner, Clark, & Clark, 2013). Our analysis of the temperature, precipitation, and solar radiation records during the 11.5 years before and after the first measurement indicates that conditions were not significantly different, and that the temporal component of the space-for-time substitution is unlikely to have been violated by changes in these variables. However, the use of 10-year age classes means that there is a potential for large variation within each class simply due to variability in the age of forests within our age classes.

Some amount of non-random spatial variation in factors affecting secondary succession is likely in any forest landscape due to spatial structure in parent material, soil nutrient status, and land-use history (Clark, Clark, & Read, 1998; Helmer, 2000). Secondary forests are particularly prone to such variation because patches of differently aged forests are non-randomly situated with respect to these variables. In the gradient examined here, previous work in old-growth

forests has shown that soil nutrient status varies with topography (Clark, Clark, Brown, Oberbauer, & Veldkamp, 2002; Porder, Clark, & Vitousek, 2006) and that lowland and upland soils support forests that respond differently to drought stress (Silva et al., 2013). However, despite these caveats, the space-for-time substitution at the landscape-scale resulted in predictions that were close to the observations after 11.5 years.

Estimating the secondary forest carbon sink requires accurate measurements of AGBD growth rates. The large amount of variation observed in secondary-forest AGBD growth raises questions about whether chronosequence studies are using sufficient sample sizes (Chazdon et al., 2016; Poorter et al., 2016). A recent study assembled data from 1,468 plots across 45 Neotropical secondary forest sites and found that the average chronosequence study used 33 plots of 0.1 ha (Poorter et al., 2016). These studies underscore the significant geographical variation in rates of secondary succession in Neotropical forest, which was attributed in part to rainfall and soil factors like cation-exchange capacity (Poorter et al., 2016). An alternative hypothesis is that rates of secondary succession are poorly constrained by plots of the size and number reported in Poorter et al. (2016), and that much of this variation is due to sampling error. Our data indicate that producing an estimate of AGBD that is close to the landscape mean requires sampling an area much larger than the average Neotropical sample size (Poorter et al., 2016). Depending on the plot size used, 3–9 ha are needed for each age class to produce estimates within 10% of the landscape mean (based on 95% of plot simulations). For example, a study with 0.1 ha plots and 4 age classes could estimate the landscape mean AGBD using about 40 plots per age class, or 160 plots in total. Studies with fewer plots could provide acceptable results. For example, a study with 40–80 0.1 ha plots (10–20 plots per 10-year age class) could achieve estimates within 10% of the landscape mean (based on 80% of plot simulations). Although these estimates of required total sampling area are larger than those typically employed (Poorter et al., 2016), they are less than the requirements described by Marvin et al. (2014) for mature tropical forests, which indicate that more than 10 ha should be sampled.

Although lidar data are rapidly increasing in availability, repeated measurements from airborne lidar are still relatively uncommon in TSF. It is possible that observations from optical sensors might be able to fill this data gap. For example, Caughlin, Rifai, Graves, Asner, and Bohlman (2016) used measurements from airborne lidar in an agricultural landscape in Panama to develop generalized linear models that predict tree cover and canopy height using Landsat. These models could then be applied to Landsat time series to quantify forest regrowth over a 12-year interval (Caughlin et al., 2016). A similar study used optical satellite data from MODIS to track changes in aboveground carbon stocks initially quantified using spaceborne lidar (Baccini et al., 2017). Current and forthcoming space missions, including the NASA Global Ecosystem Dynamics Investigation (GEDI), NASA-ISRO Synthetic Aperture Radar (NISAR), and ESA P-band radar (BIOMASS), will help to overcome these challenges by producing globally representative, high-resolution measurements of ecosystem structure to quantify AGBD and carbon stocks, and how they are changing over time.

Given the challenges of producing unbiased estimates with necessarily restricted field effort, a more rigorous recommendation is that AGBD should not be quantified using field-inventory data alone during secondary succession. These estimates should be based on active remote sensing data, such as terrestrial and airborne lidar or radar, and future spaceborne lidar and radar instruments. Field measurements are essential to calibrate and validate remote sensing, but field measurements alone limit our ability to develop precise and accurate estimates of landscape change in forest structure and AGBD.

ACKNOWLEDGEMENTS

We thank Brooke Osborne, Joy Windbourne, Katherine “KC” Cushman, Michael Keller, and Daniel Piotto for their advice and suggestions on the manuscript. SP and JB received funding from an anonymous gift to Brown University for work in Brazil’s Atlantic Forest, and from the Institute at Brown for Environment and Society. RC acknowledged funding from the And W. Mellon Foundation, NSF DEB-0424767, NSF DEB-0639393, NSF DEB-1147429. JRK was supported by NSF DEB-1357097.

AUTHOR CONTRIBUTIONS

JMB, SP, and JRK conceived the study, conducted the statistical analyses, and wrote the manuscript with help from all authors. JRK, MAH, and JBB analyzed the lidar data, RLC provided guidance on forest age determination.

ORCID


Justin M. Becknell http://orcid.org/0000-0003-2725-8215

REFERENCES

Aide, T. M., Zimmerman, J. K., Pascarella, J. B., Rivera, L., & Marcano Vega, H. (2000). Forest regeneration in a chronosequence of tropical abandoned pastures: Implications for restoration ecology. *Restoration Ecology*, *8*, 328–338. https://doi.org/10.1046/j.1526-100x.2000.80048.x

Arroyo-Rodríguez, V., Melo, F. P., Martínez-Ramos, M., Bongers, F., Chazdon, R. L., Meave, J. A., & Tabarelli, … M. (2015). Multiple successional pathways in human-modified tropical landscapes: New insights from forest succession, forest fragmentation and landscape ecology research. *Biological Reviews*, *92*, 326–340.

Baccini, A., Walker, W., Carvalho, L., Farina, M., Sulla-Menashe, M., & Houghton, R. A. (2017). Tropical forests are a net carbon source based on aboveground measurements of gain and loss. *Science*, *358*, 230–234. https://doi.org/10.1126/science.aam5962

Becknell, J. M., & Powers, J. S. (2014). Stand age and soils as drivers of plant functional traits and aboveground biomass in secondary tropical dry forest. *Canadian Journal of Forest Research*, *44*, 604–613. https://doi.org/10.1139/cjfr-2013-0331

Blair, J. B., & Hofton, M. A. (1999). Modeling laser altimeter return waveforms over complex vegetation using high-resolution elevation data. *Geophysical Research Letters*, *26*, 2509–2512. https://doi.org/10.1029/1999gl010484

Caughlin, T. T., Rifai, S. W., Graves, S. J., Asner, G. P., & Bohlman, S. A. (2016). Integrating LiDAR-derived tree height and Landsat satellite reflectance to estimate forest regrowth in a tropical agricultural landscape. *Remote Sensing in Ecology and Conservation*, *2*, 190–203. https://doi.org/10.1002/rse2.33

Chazdon, R. L. (2003). Tropical forest recovery: Legacies of human impact and natural disturbances. *Perspectives in Plant Ecology Evolution and Systematics*, *6*, 51–71. https://doi.org/10.1078/1433-8319-00042

Chazdon, R. L. (2014). *Second growth*. Chicago, IL: University of Chicago Press. https://doi.org/10.7208/chicago/9780226118109.001.0001

Chazdon, R. L., Broadbent, E. N., Rozendaal, D. M., Bongers, F., Zambrano, A. M. A., Aide, T. M., … Craven, D. (2016). Carbon sequestration potential of second-growth forest regeneration in the Latin American tropics. *Science Advances*, *2*, e1501639. https://doi.org/10.1126/sciadv.1501639

Clark, D. B., Clark, D. A., Brown, S., Oberbauer, S. F., & Veldkamp, E. (2002). Stocks and flows of coarse woody debris across a tropical rain forest nutrient and topography gradient. *Forest Ecology and Management*, *164*, 237–248. https://doi.org/10.1016/s0378-1127(01)00597-7

Clark, D. B., Clark, D. A., & Read, J. M. (1998). Edaphic variation and the mesoscale distribution of tree species in a neotropical rain forest. *Journal of Ecology*, *86*, 101–112. https://doi.org/10.1046/j.1365-2745.1998.00238.x

Drake, J. B., Dubayah, R. O., Clark, D. B., & Knox, R. G. (2002). Estimation of tropical forest structural characteristics using large-footprint lidar. *Remote Sensing of Environment*, *79*, 305–319. https://doi.org/10.1016/s0034-4257(01)00281-4

Dubayah, R. O., Sheldon, S. L., Clark, D. B., Hofton, M. A., Blair, J. B., Hurtt, G. C., & Chazdon, R. L. (2010). Estimation of tropical forest height and biomass dynamics using lidar remote sensing at La Selva, Costa Rica. *Journal of Geophysical Research*, *115*, G2.

FAO (2015). *Global Forest Resources Assessment 2015: How are the world's forests changing?*. Rome, Italy: Food and Agriculture Organization of the United Nations.

Feldpausch, T. R., da Conceicao Prates-Clark, C., Fernandes, E. C. M., & Riha, S. J. (2007). Secondary forest growth deviation from chronosequence predictions in central Amazonia. *Global Change Biology*, *13*, 967–979. https://doi.org/10.1111/j.1365-2486.2007.01344.x

Getzin, S. H., Fischer, R., Knapp, K., & Huth, A. (2017). Using airborne LiDAR to assess spatial heterogeneity in forest structure on Mount Kilimanjaro. *Landscape Ecology*, *32*, 1881–1894. https://doi.org/10.1007/s10980-017-0550-7

Helmer, E. H. (2000). The landscape ecology of tropical secondary forest in Montane Costa Rica. *Ecosystems*, *3*, 98–114. https://doi.org/10.1007/s100210000013

Johnson, E. A., & Miyanishi, K. (2008). Testing the assumptions of chronosequences in succession. *Ecology Letters*, *11*, 419–431. https://doi.org/10.1111/j.1461-0248.2008.01173.x

Kellner, J. R., Clark, D. B., & Hofton, M. A. (2009). Canopy height and ground elevation in a mixed-land-use lowland Neotropical rain forest landscape. *Ecology*, *90*, 3274. https://doi.org/10.1890/09-0254.1

Kellner, J. R., Clark, D. B., & Hubbell, S. P. (2009). Pervasive canopy dynamics produce short-term stability in a tropical rain forest landscape. *Ecology Letters*, *12*, 155–164. https://doi.org/10.1111/j.1461-0248.2008.01274.x

Kennard, D. (2002). Secondary forest succession in a tropical dry forest: Patterns of development across a 50-year chronosequence in lowland Bolivia. *Journal of Tropical Ecology*, *18*, 53–66. https://doi.org/10.1017/s0266467402002031

Lasky, J. R., Uriarte, M., Boukili, V. K., Erickson, D. L., John Kress, W., & Chazdon, R. L. (2014). The relationship between tree biodiversity and biomass dynamics changes with tropical forest succession. *Ecology Letters*, *17*, 1158–1167. https://doi.org/10.1111/ele.12322

Letcher, S. G., & Chazdon, R. L. (2009). Rapid recovery of biomass, species richness, and species composition in a forest chronosequence in Northeastern Costa Rica. *Biotropica*, *41*, 608–617. https://doi.org/10.1111/j.1744-7429.2009.00517.x

Marvin, D. C., Asner, G. P., Knapp, D. E., Anderson, C. B., Martin, R. E., Sinca, F., & Tupayachi, R. (2014). Amazonian landscapes and the bias in field studies of forest structure and biomass. *Proceedings of the National Academy of Sciences*, *111*, E5224–E5232. https://doi.org/10.1073/pnas.1412999111

Maza-Villalobos, S., Balvanera, P., & Martínez-Ramos, M. (2011). Early regeneration of tropical dry forest from abandoned pastures: Contrasting chronosequence and dynamic approaches. *Biotropica*, *43*, 666–675. https://doi.org/10.1111/j.1744-7429.2011.00755.x

McDade, L. A., Bawa, K. S., Hespenheide, H. A., & Hartshorn, G. S. (Eds.) (1993). *La Selva: Ecology and natural history of a Neotropical rain forest*. Chicago, IL: University of Chicago Press.

Mora, F., Martínez-Ramos, M., Ibarra-Manríquez, G., Pérez-Jiménez, A., Trilleras, J., & Balvanera, P. (2014). Testing chronosequences through dynamic approaches: Time and site effects on tropical dry forest succession. *Biotropica*, *47*, 38–48.

Neumann, M., Saatchi, S. S., & Clark, D. B. (2012). Quantifying spatial and temporal dynamics of tropical forest structure using high resolution airborne lidar. *Geoscience and Remote Sensing Symposium (IGARSS), 2012 IEEE International* (pp. 1664–1667). IEEE. https://doi.org/10.1109/igarss.2012.6351207

Norden, N., Angarita, H. A., Bongers, F., Martínez-Ramos, M., Granzow-de la Cerda, I., Van Breugel, M., … Finegan, B. (2015). Successional dynamics in Neotropical forests are as uncertain as they are predictable. *Proceedings of the National Academy of Sciences*, *112*, 8013–8018. https://doi.org/10.1073/pnas.1500403112

Pan, Y., Birdsey, R. A., Fang, J., Houghton, R., Kauppi, P. E., Kurz, W. A., … Ciais, P. (2011). A large and persistent carbon sink in the world's forests. *Science*, *333*, 988–993. https://doi.org/10.1126/science.1201609

Poorter, L., Bongers, F., Aide, T. M., Zambrano, A. M. A., Balvanera, P., Becknell, J. M., … Craven, D. (2016). Biomass resilience of Neotropical secondary forests. *Nature*, *530*, 211–214. https://doi.org/10.1038/nature16512

Porder, S., Clark, D. A., & Vitousek, P. M. (2006). Persistence of rock-derived nutrients in the wet tropical forests of La Selva, Costa Rica. *Ecology*, *87*, 594–602. https://doi.org/10.1890/05-0394

R Development Core Team. (2017). *R: A language and environment for statistical computing*. Vienna, Austria: R Foundation for Statistical Computing. Retrieved from http://www.r-project.org.

Rozendaal, D. M. A., & Chazdon, R. L. (2015). Demographic drivers of tree biomass change during secondary succession in northeastern Costa Rica. *Ecological Applications*, *25*, 506–516. https://doi.org/10.1890/14-0054.1

Rozendaal, D. M., Chazdon, R. L., Arreola-Villa, F., Balvanera, P., Bentos, T. V., Dupuy, J. M., … Lohbeck, M. (2017). Demographic drivers of aboveground biomass dynamics during secondary succession in Neotropical dry and wet forests. *Ecosystems*, *20*, 340–353. https://doi.org/10.1007/s10021-016-0029-4

Silva, C. E., Kellner, J. R., Clark, D. B., & Clark, D. A. (2013). Response of an old-growth tropical rainforest to transient high temperature and drought. *Global Change Biology*, *19*, 3423–3434.

Thomas, R. Q., Kellner, J. R., Clark, D. B., & Peart, D. R. (2013). Low mortality in tall tropical trees. *Ecology*, *94*, 920–929. https://doi.org/10.1890/12-0939.1

Tropical Ecology Assessment and Monitoring (TEAM) Network of Conservation International. (2009). Small-footprint, discrete return lidar

dataset collected over La Selva by Northrop Grumman Corporation through the Global Climate Monitoring Systems and 3001 remote sensing division. Retrieved from: http://www.teamnetwork.org/data/lidar

SUPPORTING INFORMATION

Additional Supporting Information may be found online in the supporting information tab for this article.

How to cite this article: Becknell JM, Porder S, Hancock S, et al. Chronosequence predictions are robust in a Neotropical secondary forest, but plots miss the mark. *Glob Change Biol*. 2018;24:933–943. https://doi.org/10.1111/gcb.14036